

Geometry Design of an Elastic Finger-Shaped Sensor for Estimating Friction Coefficient by Pressing an Object

Takashi Maeno and Tomoyuki Kawamura

Department of Mechanical Engineering
Keio University, Yokohama 223-8522 JAPAN
e-mail: maeno@mech.keio.ac.jp, kawamura@2000.jukuin.keio.ac.jp

Abstract - Authors have proposed a method for detecting a friction coefficient between a planar object and an elastic finger-shaped sensor by only pressing the sensor against the object in our previous study. In the present study, an elastic finger-shaped sensor made of silicone rubber is designed and produced. First, geometry of the finger-shaped sensor is designed using finite element analysis (FEA). Results of FEA revealed that strain detected using strain gage incorporated near the edge of the contact surface varies when the friction coefficient between the finger-shaped sensor and a planar object varies. Then, in an experiment using the newly designed sensor, it is confirmed that the friction coefficient between the finger and the object is detected using the strain inside the finger when the sensor is pressed against the object.

1. INTRODUCTION

One of the most important problems in the field of robotics is that of developing a robot hand which is able to grip and lift an object avoiding slippage and crushing even when the weight and friction coefficients are unknown. Several methods for lifting objects have been proposed. These can be classified into the following three types. The first method type involves detecting the microvibration of a finger when the object starts slipping [1]-[4]. However, this method produces a slippage and is not adequate for precise positioning because the object moves slightly in the lifting direction. The second method type involves detection of partial incipient slippage between a finger and an object. The partial slippage refers to the contact condition between two bodies for which part of the contact area "slips" and the other part "sticks" or "adheres". Tremblay et al [5] proposed detection of a localized slip between a sensor and an object which precedes gross slip. They detected the vibration due to the localized slip using two acceleration sensors and estimated the friction coefficient using the ratio of the tangential and normal force. Using this method, they could clearly detect the incipient slippage, however, the value of the estimated friction coefficient is not accurate. Canepa [6] and Maeno [7] detected the partial incipient slippage of the object using a skin-like sensor. They utilized the distribution

pattern of the stress/strain inside the elastic finger to detect the partial slip information. This is similar to what human beings do [8]. However, this method requires a large number of sensors incorporated in an elastic body and a pattern recognition technique. The third method type involves estimation or direct measurement of the friction coefficient between the object and finger. Bicchi [9][10] estimated the friction coefficient between a force-torque tactile sensor and the object. However, the estimated value of the friction coefficient is obtained after the entire slippage occurs. Yamada [11] presented a method for measuring a friction coefficient directly by rotating a disk placed in a robot hand. This method is useful because the normal and tangential forces are easily controlled so as to avoid slippage by using the friction cone between two objects calculated from the measured friction coefficient. However, the equipment becomes large and heavy. As described above, detection of a friction coefficient is important for a robot hand to be able to grip and lift an object while avoiding slippage and crushing. A method is required for obtaining the friction coefficient without entire slippage and using a simple sensor.

On the other hand, human beings can grip and lift an object even when the weight and the friction coefficient are unknown. How are we able to do this? Johansson [8] measured the nerve signals and normal/tangential force simultaneously when human fingers gripped and lifted several kinds of flat objects. It was shown that the frequency of nerve signals just after the time the finger touched the object differs when the friction coefficient between the finger and object differs. When the friction coefficient is small, i.e. in the case of silk, frequency of the nerve signal is large. Conversely, when the friction coefficient is large, i.e. in the case of sandpaper, frequency of the nerve signal is small. We can conclude that the difference of the frictional coefficient is already distinguished slightly after the time the fingers are in contact with the object. From this, we can predict that the friction coefficient between an artificial finger and object can be detected only by indenting the object into an artificial finger-shaped elastic sensor. Shinoda [12][13] showed that tangential stress/strain at the center of the elastic finger indicates the difference in friction coefficient when the elastic finger is pressed against a planar object.

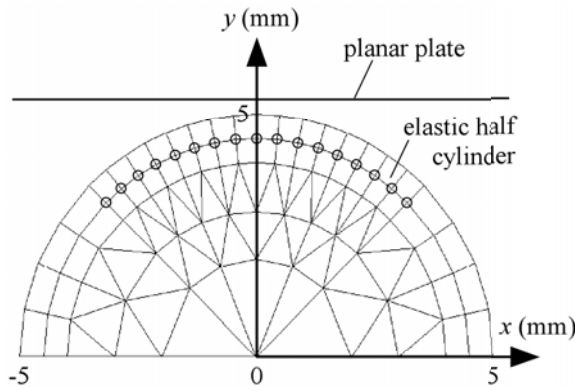


Fig. 1 Finite element model of the cross-section of a simple half-cylindrical finger

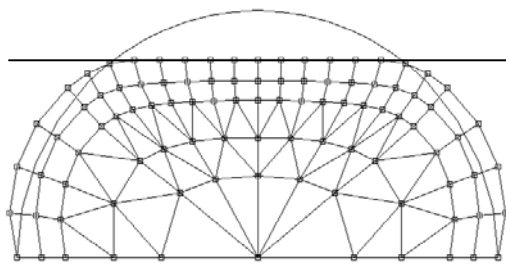


Fig. 2 Deformation of an elastic finger when a plate is indented into the finger by 1 mm

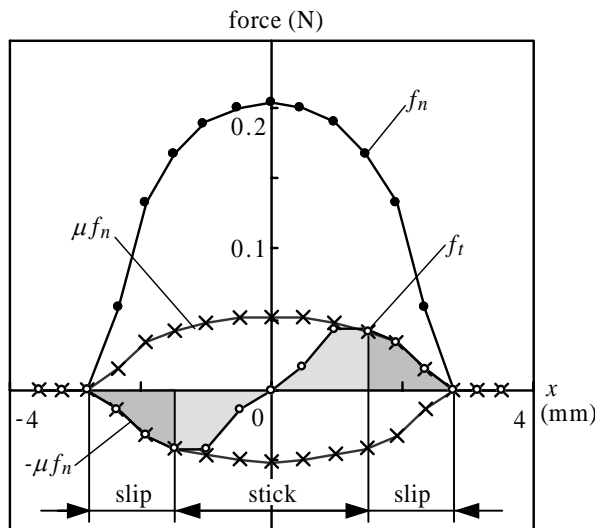


Fig. 3 Reaction force distribution when the plate is indented into the elastic finger by 1 mm ($\mu=0.25$)

Authors [14] also showed that shear stress/strain distribution of a half cylindrical finger indicates the difference in friction coefficient. However, the geometry of the elastic finger were not optimized in both methods. In the present study an elastic finger-shaped sensor made of silicone rubber, in which strain gages are incorporated near the edge of the contact region, is designed in detail using finite element analysis (FEA). The locations and angles of strain gages are determined such that the strain varies when the friction coefficient varies. Finally, an experiment is performed using the produced finger-shaped sensor in order to verify the proposed sensor.

2. METHOD

2.1. Model

Contact between an elastic finger having a curved surface and a planar object was analyzed by authors [14] using the finite element method (FEM). Figure 1 shows a FE (finite element) model of a simple half-cylindrical finger with a radius of 5 mm. The normal load is changed by increasing the forced displacements of the planar plate in the y -direction by 0.1 mm in one time interval until the displacement reaches 1 mm. The nodes at $y=0$ are constrained in the x - and y -directions. The FE model consists of 96 nodes and 108 elements. The elastic modulus of the finger is 1 MPa. Nonlinearity due to large deformation is neglected.

2.2. Results

Figure 2 shows the deformation of the elastic finger when the planar plate is indented into the elastic finger by 1 mm in the direction normal to the finger surface. Figure 3 shows a normal and tangential contact force distribution at the surface of the cylindrical finger when a forced displacement of the plate in the y -direction is 1 mm and the friction coefficient μ is 0.25.

The distribution of normal force f_n is semi-circular because the finger is curved. The tangential force f_t , i.e. the friction force, has a local minimum and a local maximum. The sum of the tangential force is always zero because no movement of the plate in the x -direction is applied. Two slip regions at the edge of the contact and a stick region at the center of the contact are produced. This is because the limiting friction force is small at the edge of the contact. When the indentation is increased, the tangential reaction force or friction force reaches the limiting friction force near the edges of the contact. Then these regions slip and a kinetic friction force is applied. The partial incipient slip regions at both edges of the contact region changes when the indentation is changed.

Figure 4 shows the normal strain distribution, ϵ_x , ϵ_y , and the shear strain distribution, γ_{xy} inside the elastic finger at the nodes shown as circles in Fig. 1 when a plate is indented into the elastic finger by 1 mm and the friction coefficient is changed from 0.06 to 1.0. The distribution

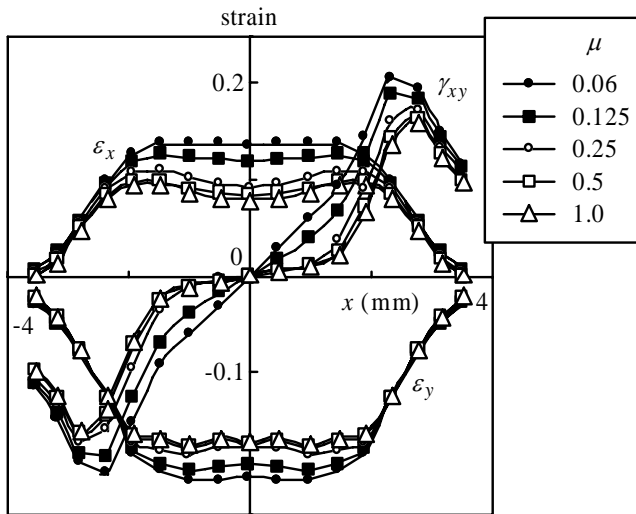


Fig. 4 Strain distribution when the plate is indented into the elastic finger by 1 mm for various frictional coefficients

patterns of the normal strains ϵ_x and ϵ_y do not change noticeably. On the other hand, the distribution pattern of the shear strain γ_{xy} changes as a function of the variation in the friction coefficient. Shinoda [12][13] used the slight change in tangential stress/strain at $x=0$ to estimate the friction coefficient. The changes in tangential stress/strain, however, were not large because the effect of the slip area at the edge of the contact area on the change in tangential stress/strain at $x=0$ is not large. Therefore, authors [14] concluded that the shear stress/strain should be used to detect the friction coefficient rather than the tangential stress/strain.

3. FE ANALYSIS FOR GEOMETRY DESIGN

3.1. Model

Recently, several kinds of sensors for measuring the shear strain have been proposed [7][12][15], and these sensors can be used to obtain shear strain for detecting the friction coefficient. The simplest technique for detecting the shear strain is to measure the tensile strain using an inclined strain gage incorporated inside the elastic body. We therefore design a finger-shaped sensor made of silicone rubber, which has strain gages incorporated inside.

The half cylindrical model used in the previous section does not have an optimum geometry with maximized sensitivity for detecting the friction coefficient, particularly when the friction coefficient is large. We therefore design in detail the geometry of the sensor used to detect the friction coefficient up to a large value by calculating the contact condition between the finger-shaped sensor and a flat object. The effects of location and angle of the strain gage are also calculated in

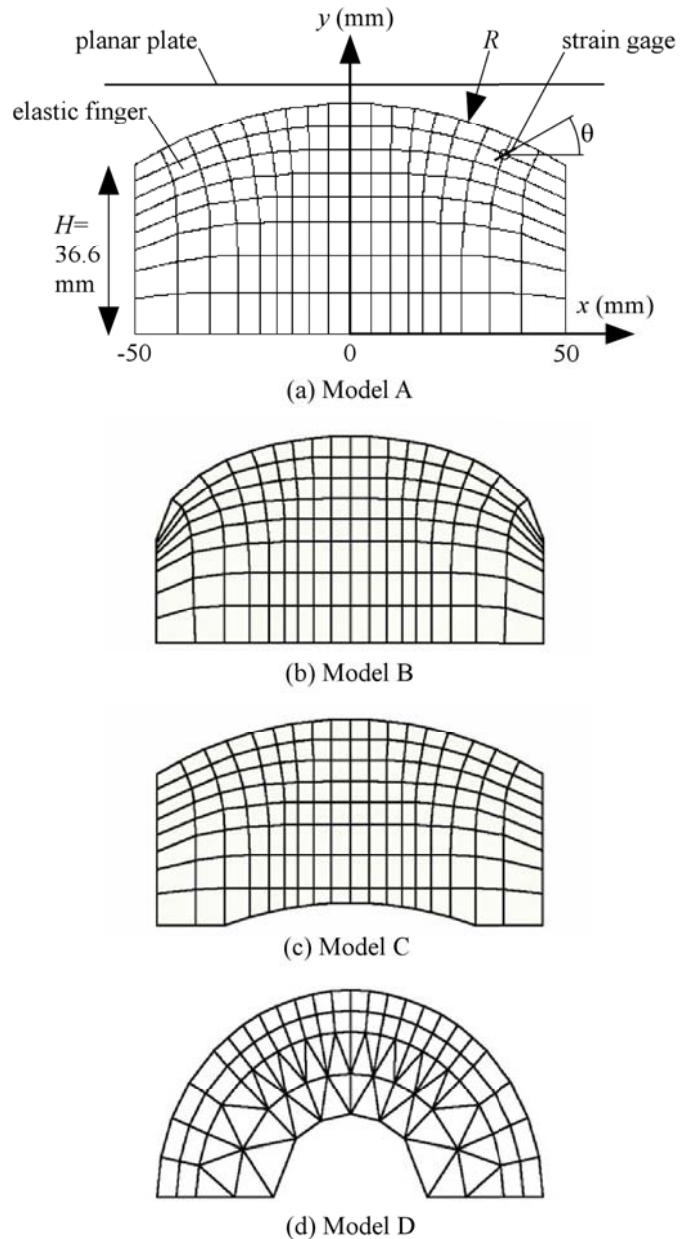


Fig. 5 Finite element model of the cross-section of the elastic finger

order to determine the location and angle which provide the maximum sensitivity for detecting the friction coefficient.

In addition to the half cylindrical model, we also performed calculation using half cylinders with sections removed from the corners (See Fig. 5(a)), cylinders having variable radius (b), cylinders having removed sides and removed core at the bottom (c), and half cylinders having core at the bottom (d), in order to investigate the effect of geometry. The radius of the cylinder R and the height of

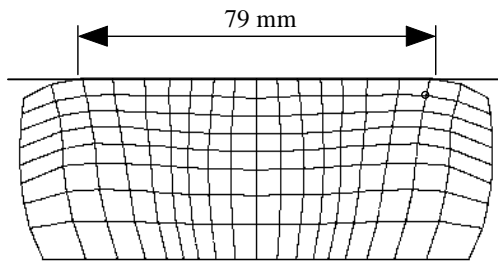


Fig. 6 Deformation of the newly designed elastic finger when a plate is indented into the finger by 10 mm

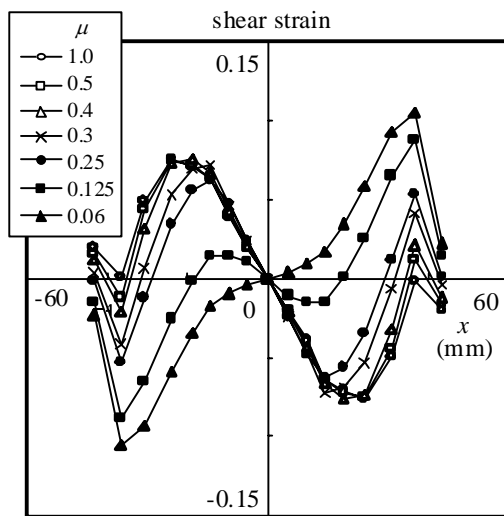


Fig. 7 Shear strain distribution of the newly designed finger-shaped sensor

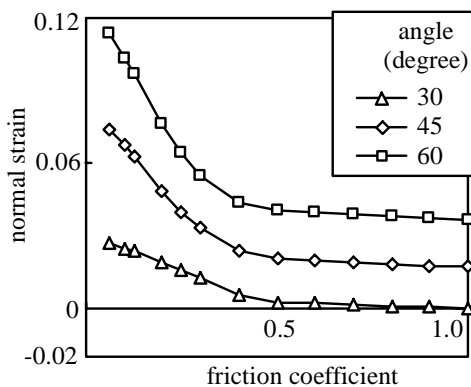


Fig. 8 Calculated normal strain of strain gages when angle of the strain gage at $x=36$ mm is changed

the removed area H are set as variables in the calculation for the model A. Similarly, peculiar length of the models are set as variables for models B to D. The indentation depth is fixed at 10 mm in the calculation. In addition, plane strain elements are used, and non-linearity due to large deformation is neglected. The nodes at $y=0$ are constrained in the x - and y -directions.

3.2. Results

FE analysis for different geometries revealed that a cylinder having a radius of 100 mm and an edge height of 36.6 mm, as shown in Fig. 5(a), was the most sensitive to the change in the friction coefficient throughout a large range when the depth of indentation is 10 mm. Figure 6 shows the deformation of the elastic finger when a planar plate is indented for 10 mm. The contact width is approximately 79 mm. Figure 7 shows variation of shear strain with the friction coefficient. Comparison with Fig. 4 reveals that the change in shear strain for different friction coefficient is larger in Fig. 7. In particular, shear strain changes even when the friction coefficient is large at the node $x=36$ mm which is indicated by a circle in Figs. 5 and 6. This is because the position $x=36$ mm is near the edge of the contact area. The area near the edge of contact slips easily because both sides of the finger have been removed. Figure 8 shows the change in normal strain at the node where $x=36$ mm when the angle of strain gage with respect to the horizontal line, θ (see Fig. 5), is changed. The normal strain in inclined axis acts similar to shear strain. The strain is large when the angle is large; however, when the angle is 30 degree the relationship between friction coefficient and strain is linear even when the friction coefficient is large. Thus, the change in friction coefficient can be estimated via the normal strain measured using a strain gage located at $x=36$ mm at an angle of 30 degrees.

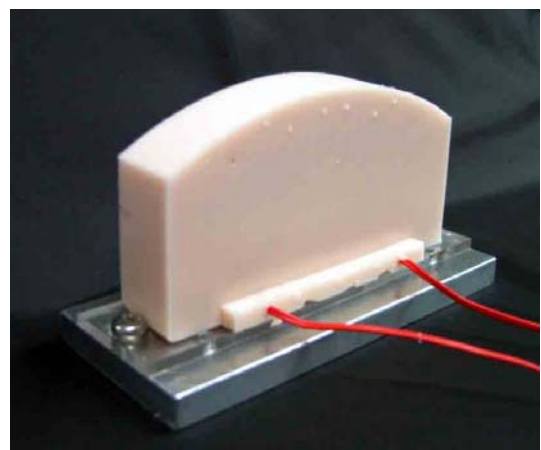


Fig. 9 Newly designed elastic finger-shaped sensor

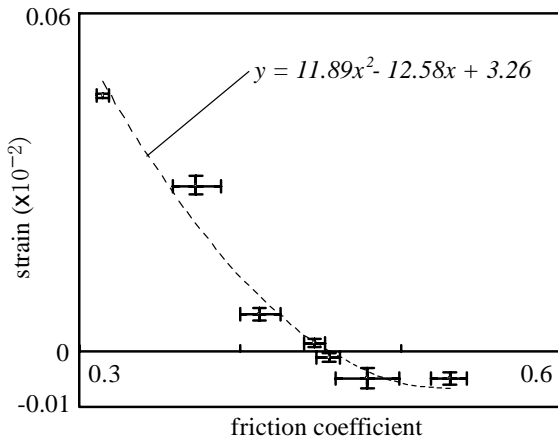


Fig. 10 Relationship between friction coefficient and measured strain

4. DEVELOPMENT AND MEASUREMENT

The designed finger-shaped sensor is made using silicone rubber and a strain gage. Figure 9 shows the newly developed sensor. The strain gage is embedded directly inside the silicone rubber at the location shown in Fig. 5 (a). The width of the sensor is 20 mm. Seven objects having planar surfaces are prepared. The friction coefficients between these surfaces and the finger-shaped sensor are then measured in advance. Then the strain of the finger-shaped sensor is measured when the sensor is pressed against the surface of the planar object for 10 mm. Ten measurements are performed for each object. The relationship between the measured friction coefficient and the strain is shown in Fig. 10. The line in Fig. 10 indicates a second-order equation for approximating the seven points. Vertical and horizontal bars around the measured points represent standard deviation. The figure shows the difference in friction coefficient for the seven objects. In addition, the strain is small when the friction coefficient is large, which is also the case in Fig. 8. The largest standard deviation of strain is 1.5×10^{-4} . The error of the friction coefficient using the second-order equation and the standard deviation is 0.1. The minimum value of the equation is at about $\mu=0.5$. Hence, the friction coefficient can be measured with an accuracy of 0.1, up to 0.5 using the newly developed finger-shaped sensor. Thus, the proposed method is confirmed using actual equipment. Although the accuracy is not satisfactory, repeatability, accuracy of the sensor geometry, and the condition of the surface, can improve the performance of the sensor.

5. CONCLUSIONS

We have proposed the geometry of the finger-shaped sensor having a curved surface for detecting the friction

coefficient between an object and the sensor when the sensor is pressed against the object. The contact problem is solved between the newly designed sensor and plates having different friction coefficients when the plate is indented into the sensor. The strain detected using the strain gage incorporated near the contact edge between the sensor and the object is useful to estimate the friction coefficient between the two bodies. Then the elastic sensor is produced in order to verify the correctness of the FE simulation and to demonstrate that the friction coefficient can be estimated.

REFERENCES

- [1] R. W. Patterson et al., "The Induced Vibration Touch Sensor - a New Dynamic Touch Sensing Concept", *Robotica*, Vol. 4, 1986, pp. 27-31.
- [2] D. Dornfeld et al., "Slip Detection Using Acoustic Emission Signal Analysis," *Proc. IEEE Int. Conf. Robotics Automation*, 1987, pp. 1868-1875.
- [3] R. D. Howe and M. R. Cutkosky, "Sensing Skin Acceleration for Slip and Texture Perception", *Proc. IEEE Int. Conf. Robotics Automation*, 1989, pp. 145-160.
- [4] P. Dario et al., "Planning and Expecting Tactile Exploratory Procedures", *Proc. IEEE/RSJ Int. Conf. on Intelligent Robotics Systems*, 1992, pp. 1896-1903.
- [5] M. Tremblay and M. R. Cutkosky, "Estimating Friction Using Incipient Slip Sensing During a Manipulation Task", *Proc. IEEE Int. Conf. Robotics Automation*, 1993, pp. 429-434.
- [6] G. Canepa, D. D. Rossi et al, "Detection of Incipient Object Slippage by Skin-Like Sensing and Neural Network Processing", *IEEE Trans. Systems, Man, Cybernetics-Part B*, vol. 28, no. 3, 1998, pp. 348-356.
- [7] T. Maeno et al, "Analysis and Design of a Tactile Sensor Detecting Strain Distribution inside an Elastic Finger", *Proc. IEEE/RSJ Int. Conf. on Intelligent Robotics Systems*, 1998, pp. 1658-1663.
- [8] S. Johansson and G. Westling, "Signals in Tactile Afferents from the Fingers Eliciting Adaptive Motor Responses during the Precision Grip", *Exp. Brain Res.*, vol. 66, 1988, pp. 141-154.
- [9] A. Bicchi, "Intrinsic Contact Sensing for Soft Fingers", *Proc. IEEE Int. Conf. Robotics Automation*, vol. 2, 1990, pp. 968-973.
- [10] A. Bicchi, J. K. Salisbury and D. L. Brock, "Experimental Evaluation of Friction Data with an Articulated Hand and Intrinsic Contact Sensors, " *Experimental Robotics-II*, R. Chatila and G. Hirzinger (Eds.) . *Lecture Notes in Control and Information Sciences*, vol.190, Springer--Verlag, 1994, pp. 153-167.
- [11] Y. Yamada et al., "Active Sensing of Static Friction Coefficient", *Proc. '93 ICAR*, 1993, pp. 185-190.

- [12] H. Shinoda et al., "Instantaneous Evaluation of Friction Based on ARTC Tactile Sensor", Proc. IEEE Int. Conf. Robotics Automation, 2000, pp. 2173-2178.
- [13] S. Sasaki, W. H. Sheong and H. Shinoda, Instantaneous Detection of the Friction Coefficient Using ARTC Tactile Sensor, Proc. SICE, Vol. 33. No. 4, 1999, pp. 339-340 (in Japanese).
- [14] S. Cheng, T. Kawai and T. Maeno, Detection of Friction Coefficient using Strain Distribution of semicircular Elastic Finger, Proc. 1999 JSME Annual Meeting (V), No. 99-1, 1999, pp. 235-236 (in Japanese).
- [15] H. Shinoda, K. Matsumoto and S. Ando, "Acoustic Resonant Tensor Cell for Tactile Sensing", Proc. IEEE Int. Conf. Robotics Automation, 1997, pp. 3087-3092.